Ex Vivo Programming of Dendritic Cells by Mitochondria-Targeted Nanoparticles to Produce Interferon-Gamma for Cancer Immunotherapy

Sean Marrache,[†,⊥] Smanla Tundup,[§,⊥] Donald A. Harn,[§] and Shanta Dhar[†,‡,*]

[†]NanoTherapeutics Research Laboratory, Department of Chemistry, and [‡]Department of Physiology and Pharmacology, University of Georgia, Athens, Georgia 30602, United States and [§]Department of Infectious Diseases, College of Veterinary Medicine, University of Georgia, Athens, Georgia 30602, United States. [⊥]S. Marrache and S. Tundup contributed equally.

ABSTRACT One of the limitations for clinical applications of dendritic cell (DC)-based cancer immunotherapy is the low potency in generating tumor antigen specific T cell responses. We examined the immunotherapeutic potential of a mitochondria-targeted nanoparticle (NP) based on a biodegradable polymer and zinc phthalocyanine (ZnPc) photosensitizer (T-ZnPc-NPs). Here, we report that tumor antigens generated from treatment of breast cancer cells with T-ZnPc-NPs upon light stimulation activate DCs to produce high levels of interferon-gamma, an important cytokine considered as a product of T and natural killer cells. The remarkable *ex vivo* DC stimulation ability of this tumor cell supernatant is a result of an interleukin (IL)-12/IL-18 autocrine effect. These findings contribute to the understanding of how *in situ* light activation amplifies the host immune responses when NPs deliver the photosensitizer to the mitochondria and open up the possibility of using mitochondria-targeted-NP-treated, light-activated cancer cell supernatants as possible vaccines.

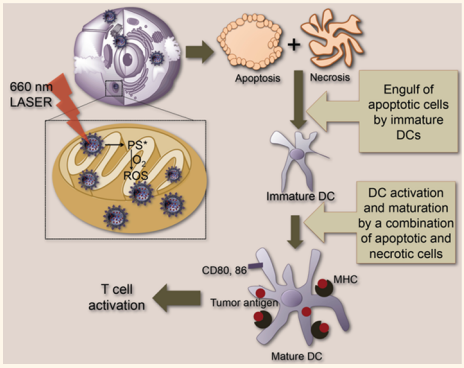

KEYWORDS: vaccine · photodynamic therapy · dendritic cell therapy · biodegradable polymer · apoptosis

A host's dysfunctional immune system assists tumors in evading immunosurveillance.[1] However, the immune system when properly stimulated can eradicate cancer cells.[2] Tumor immunity involves interactions of cytokines and effector cells. One cytokine that plays a central role in coordinating tumor immune responses is interferon-gamma (IFN-γ). Immature dendritic cells (iDCs) secrete cytokines to initiate and enhance both innate and acquired immunity, detect and capture antigens, undergo a maturation process, and prime immune responses by activating naïve T cells. Use of DCs for clinical cancer immunotherapy is extremely attractive.[3,4] DCs are professional antigen-presenting cells (APCs), which possess the entire array of antigen-presenting and co-stimulatory molecules. One of the major limitations for clinical application of DCs is the low potency in generating tumor antigen specific $CD8^+$ T cell responses *in vivo*.[5,6] Infectious agents activate DCs to secret interleukin (IL)-12, which subsequently induces IFN-γ production by natural killer (NK) cells and directs T helper cell type 1 (Th1) development. We hypothesized that *ex vivo* engineering of DCs to produce IFN-γ for increased T cell activity and development of a Th1-type immune response can serve as an alternative therapeutic modality for metastatic cancer. Photodynamic therapy (PDT), an antitumor therapeutic modality that has approval for the treatment of oncological diseases, involves administration of a photosensitizer (PS) followed by illumination of the tumor with long-wavelength (600−800 nm) light. PDT produces reactive oxygen species (ROS), resulting in vascular shutdown, cancer cell apoptosis, and the induction of a host immune response.[7,8] Preclinical and clinical techniques of this method of cancer treatment are still being optimized to address that PDT sometimes fails to eradicate the targeted tumor and

* Address correspondence to shanta@uga.edu.

Received for review June 21, 2013 and accepted July 30, 2013.

Published online July 30, 2013
10.1021/nn403158n

to boost immunity. We speculated that these failures may in part arise from inhomogeneous delivery of PS within the tumor, in particular the inability to reach its target organelle, the mitochondria of cells, and the inability to produce short-lived singlet oxygen ($^1O_2$) in the mitochondria of tumor cells. Those PSs that accumulate inside the mitochondria induce apoptosis upon photoirradiation, whereas those that bind to the nonmitochondrial compartments kill cells less efficiently by a nonapoptotic mechanisms. Photodynamically induced mitochondrial apoptosis induces signal transduction pathways, which participate in the development of immune responses. Thus, we conjectured that exposing DCs *ex vivo* to tumor cell supernatant generated from mitochondria-targeted light-activated cancer cells may unravel pathways that can be used to improve DC-based cancer immunotherapy. Thus we ask whether targeting mitochondria with an engineered biodegradable nanoparticle (NP) containing a mitochondria-acting PS such as zinc phthalocyanine (ZnPc),[9] induction of mitochondrial apoptosis after light stimulation, and activation of DCs *ex vivo* with cancer cell antigens can induce immunity. Polymeric NPs of poly(lactide-*co*-glycolide)-*b*-polyethyleneglycol (PLGA-*b*-PEG) block copolymers are especially promising as drug delivery vehicles.[10−16] We recently constructed a targeted functionalized polymer using PLGA-*b*-PEG and a lipophilic triphenyl phosphonium (TPP) cation[17] for mitochondria-targeted delivery of payloads.[18] Targeted NPs from PLGA-*b*-PEG-TPP take advantage of substantial negative mitochondrial inner membrane potential ($\Delta\psi_m$) to deliver cargos into mitochondria.[18] By using such an engineered vehicle to target the intracellular organelle mitochondria, we observed that DCs cultured with supernatants from breast cancer cells activated with mitochondria-targeted PDT had significant levels of IFN-γ. To the best of our knowledge this is the first report that demonstrates the ability of a mitochondria-targeted system to stimulate murine bone marrow derived DCs (BMDCs) *ex vivo* to secret IFN-γ, the most versatile player of immune activation. By highlighting the importance of mitochondria-targeted PDT of breast cancer and subsequent cytokine secretion by BMDCs receiving stimulation with mitochondria-targeted-PDT-treated cancer cells, our data provide a model considering *ex vivo* manipulation of DC function for potential clinical applications. In this report, we discuss *ex vivo* IFN-γ production pathways from DCs upon stimulation with mitochondria-targeted-PDT-activated breast tumor cell antigens (Figure 1a).

RESULTS AND DISCUSSION

Construction of Mitochondria-Targeted NPs for DC Activation. The use of mitochondria-targeted NPs for ZnPc delivery is obvious due to the fact that ZnPc acts on the mitochondria of cells and upon photoactivation generates short-lived $^1O_2$ as the cytotoxic agent to show its photodynamic activity.[19,20] The second-generation ZnPc photosensitizer has strong phototoxicity in the therapeutic window of 600−800 nm; however, the hydrophobic characteristic hinders its systemic administration and restricts its possible translation to the clinic. The active species involved in ZnPc-based PDT, $^1O_2$, has a short lifetime of <0.04 μs in biological systems and restricts its reactivity to within a radius of about 0.2 μm from its point of generation.[19,20] Our recently developed mitochondria-targeted biodegradable polymer, PLGA-*b*-PEG-TPP,[18] has the ability to encapsulate hydrophobic compounds such as ZnPc with very high efficiency. Using a nanoprecipitation method,[21,22] we were able to load high amounts of ZnPc in the polymeric core to construct targeted T-ZnPc-NPs (Figure 1b). The polymer PLGA-*b*-PEG-OH without a cationic TPP moiety allowed us to construct a nontargeted NT-ZnPc-NP that served as a control to probe the advantages of delivering ZnPc inside the mitochondria of cells. Dynamic light scattering (DLS) measurements revealed that the mean diameter of the mitochondria-targeted NPs, T-ZnPc-NPs, is ∼65 to 75 nm and they are positively charged (∼24 to 34 mV) (Figure 1c, Tables S1, S2). The size of the NT-ZnPc-NPs was found to be ∼70 nm, and they are negatively charged (∼−25 to −30 mV) (Figure 1c, Tables S1, S3). ZnPc loading and encapsulation efficiency (EE) were optimized by varying the weight percentage of ZnPc to polymer (% w/w) (Tables S2, S3). For both T-ZnPc-NPs and NT-ZnPc-NPs, percent loading increased as the percent feed was raised and then saturated as the feed reached 40%. For all studies, we used ∼10% ZnPc-loaded NPs. Transmission electron microscopy (TEM) images of the NPs showed homogeneous populations (Figure 1d). To compare the immune activation properties of PDT with chemotherapeutics, we encapsulated a mitochondria-targeting cancer chemotherapeutic lonidamine (LND)[23] in the targeted and nontargeted polymers to construct T-LND-NPs and NT-LND-NPs.[18] We studied LND release kinetics from the NPs, a necessary property to show anticancer property by inhibiting mitochondria-bound hexokinase. The amount of LND released from the NPs under physiological conditions shows an initial 19% burst release followed by a period of controlled release, reaching a value of 60% after 4 h, and most LND was released in 8 h (Figures S1, S2).

Mitochondria-Targeted Light Activation of Cancer Cells. The photodynamic activities of T-ZnPc-NPs, NT-ZnPc-NPs, and free ZnPc were investigated against human breast cancer MCF-7 and cervical cancer HeLa cells. We used human mesenchymal stem cells (hMSCs) as noncancerous controls for their ability to differentiate into other cell types and to partake in the anatomy and physiology of remote organs. None of these constructs showed any toxicity in the dark (Figure S3). Four hours following incubations with different constructs, cells

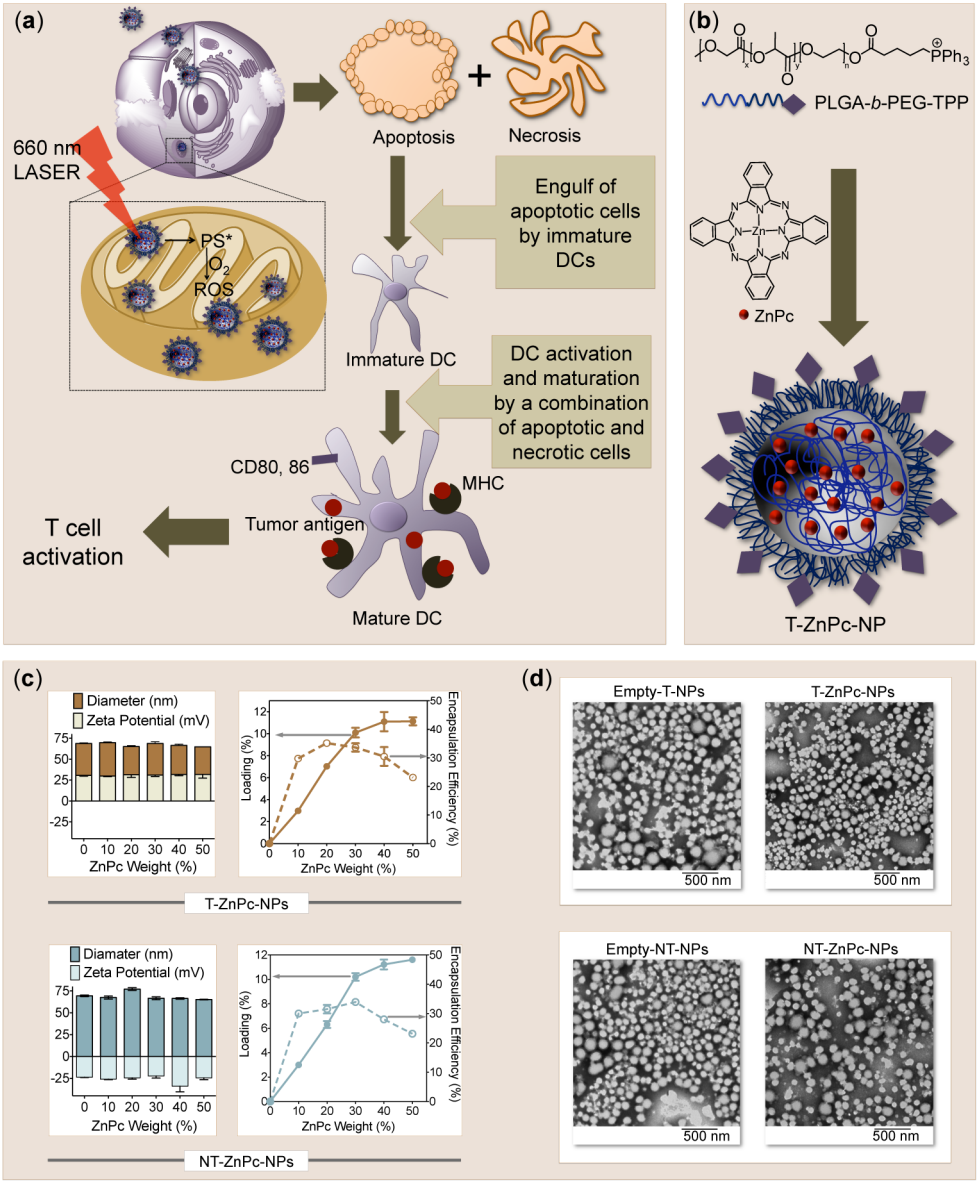

Figure 1. (a) Action of mitochondria-targeted NPs upon light activation inside the mitochondria to produce ROS, which causes cell death *via* apoptosis and necrosis. (b) Synthesis of T-ZnPc-NPs by following a nanoprecipitation method. (c) Size, zeta potential, and ZnPc loading in targeted and nontargeted NPs. (d) TEM images of targeted and nontargeted empty and ZnPc-loaded NPs.

were stimulated with a 660 nm laser light for 1 min, and viability was determined following the 3-(4,5-dimethylthiazol-2-yl)-2,5-diphenyltetrazolium bromide (MTT) assay. A higher phototoxic effect was observed with T-ZnPc-NPs in HeLa and MCF-7 cells ($IC_{50\text{-}HeLa}$: 96 ± 19 nM, $IC_{50\text{-}MCF\text{-}7}$: 49 ± 12 nM) than NT-ZnPc-NPs ($IC_{50\text{-}HeLa}$: 222 ± 59 nM, $IC_{50\text{-}MCF\text{-}7}$: 349 ± 125 nM) and free ZnPc ($IC_{50\text{-}HeLa}$: 570 ± 51 nM, $IC_{50\text{-}MCF\text{-}7}$: 406 ± 129 nM) (Figure 2a). Control cells incubated with empty-T-NPs and empty-NT-NPs did not show any cell death after illumination (Figure S3). When hMSCs were exposed to T-ZnPc-NPs, NT-ZnPc-NPs, and free ZnPc and stimulated with laser, viability was higher for the cells treated with T-ZnPc-NPs ($IC_{50\text{-}hMSC}$: 36 μM) compared to those treated with NT-ZnPc-NPs ($IC_{50\text{-}hMSC}$: 31 μM) or free ZnPc ($IC_{50\text{-}hMSC}$: 6.5 μM) (Figure 2a). An interesting observation was T-ZnPc-NP or NT-ZnPc-NP had limited toxicity in hMSC cells; however, free ZnPc significantly decreased hMSC cell viability. We believe that the greater uptake of T-ZnPc-NPs by the cancer cells with elevated $\Delta\psi_m$ is responsible for their enhanced efficiency compared to the nonmalignant hMSCs with normal $\Delta\psi_m$.[24,25] Our results suggest that T-ZnPc-NPs with nanomolar IC_{50} in cancer cells may not have an adverse effect on hMSC cells and potentially other normal cell types in the body as well.

Mitochondria-Targeted NPs Provide a Unique Mixture of Apoptotic and Necrotic Cells. Immature DCs have the unique properties of phagocytosis, processing, and presentation of tumor-associated antigens (TAA) from apoptotic

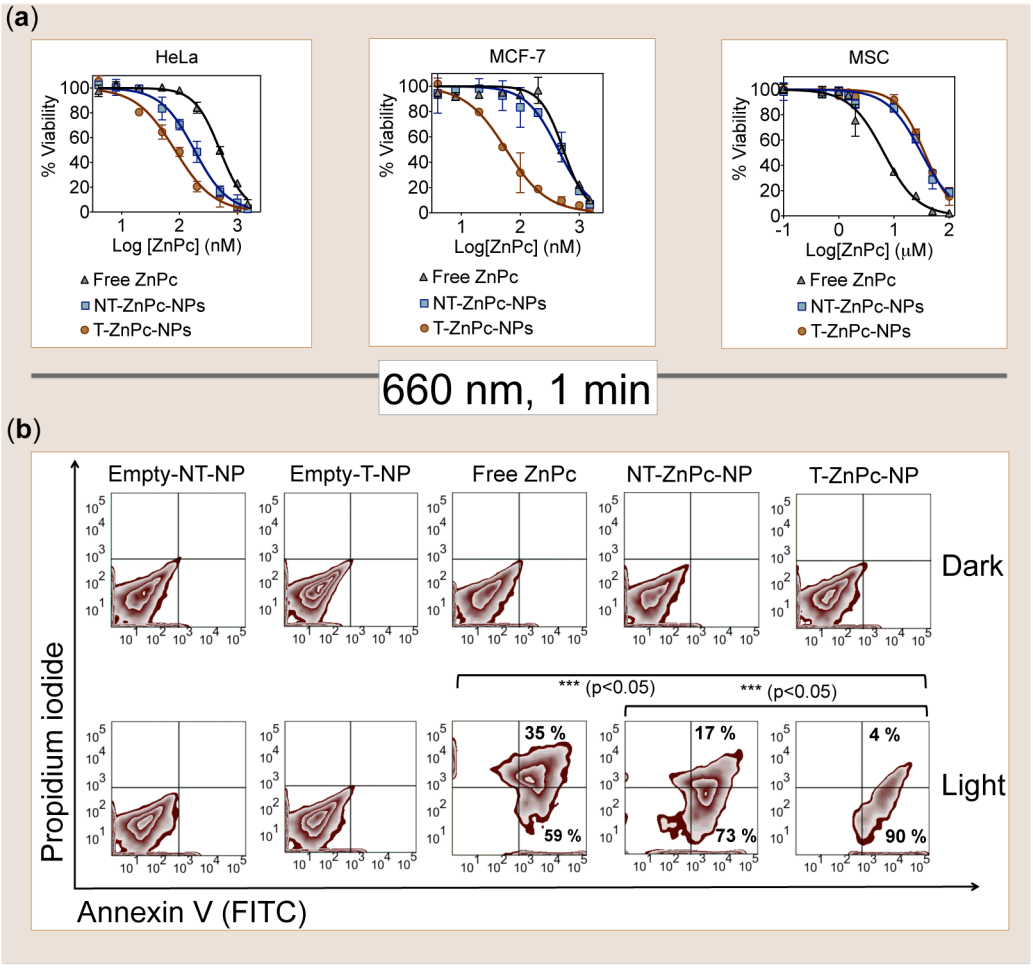

Figure 2. (a) HeLa and MCF-7 cancer cells respond differently to light activation compared to hMSC. Cells on 96-well plates were incubated for 4 h with T-ZnPc-NP, NT-ZnPc-NP, and free ZnPc. Cells were irradiated with a 660 nm laser (20 mW) for 1 min, media was changed after 12 h, cells were further incubated for additional 60 h, and viability was assessed by the MTT assay. (b) FACS analysis using annexin V-Alexa Fluor/PI staining for apoptosis detection in MCF-7 cells on treatment with T-ZnPc-NP (1 μM), NT-ZnPc-NP (1 μM), and free ZnPc (1 μM) for 16 h in the dark or irradiation with a 660 nm laser for 1 min after 4 h incubation, followed by incubation in the dark for 12 h. Cells in the lower right quadrant indicate annexin-positive/PI-negative, early apoptotic cells. The cells in the upper right quadrant indicate annexin-positive/PI-positive, late apoptotic or necrotic cells.

cancer cells for inducing potent immune responses.[26] However, optimal presentation of TAA requires not only phagocytosis of apoptotic tumor cells by iDCs but also activation and maturation of iDCs *via* exposure to the necrotic tumor cells. Therefore, a unique combination of apoptotic and necrotic tumor cells is needed for the tumor-associated DCs to induce a potent immune response. PDT-induced apoptosis can proceed through different pathways involving either an extrinsic cytoplasmic or an intrinsic mitochondrial pathway.[27] Intracellular localization of the PS coincides with the primary site of photodamage because the active species $^1O_2$ has a short lifetime and very limited diffusion in biological systems, indicating that primary molecular targets of the PDT process must reside within a few nanometers from the PS. Thus, PSs localizing in the mitochondria promote apoptosis, but PDT with PSs residing in the nonmitochondrial compartments can either delay or block the apoptotic program, predisposing the cells to necrosis. To explore the ability of T-ZnPc-NPs to induce apoptosis upon PDT, we exposed breast cancer MCF-7 cells to T-ZnPc-NPs and compared apoptosis with NT-ZnPc-NPs and free ZnPc-treated cells by the annexin-V-propidium iodide (PI) assay.

T-ZnPc-NPs strongly induced the early stage of apoptosis. In contrast, empty-T-NPs, empty-NT-NPs, and dark controls did not increase the total number of apoptotic cells (Figure 2b, Figure S4). NT-ZnPc-NPs showed less apoptotic efficacy compared with targeted NPs. Free ZnPc induced late apoptosis or necrosis to a higher extent compared with T-ZnPc-NPs and NT-ZnPc-NPs. Increased apoptotic activity of T-ZnPc-NPs may possibly be due to the unique ability of the targeted NPs to deliver ZnPc inside mitochondria, thereby triggering mitochondria-mediated cell death cascade/sequence. Apoptotic cancer cells, as a result of PDT, release antigens, which interact with and are internalized by DCs, leading to their activation,

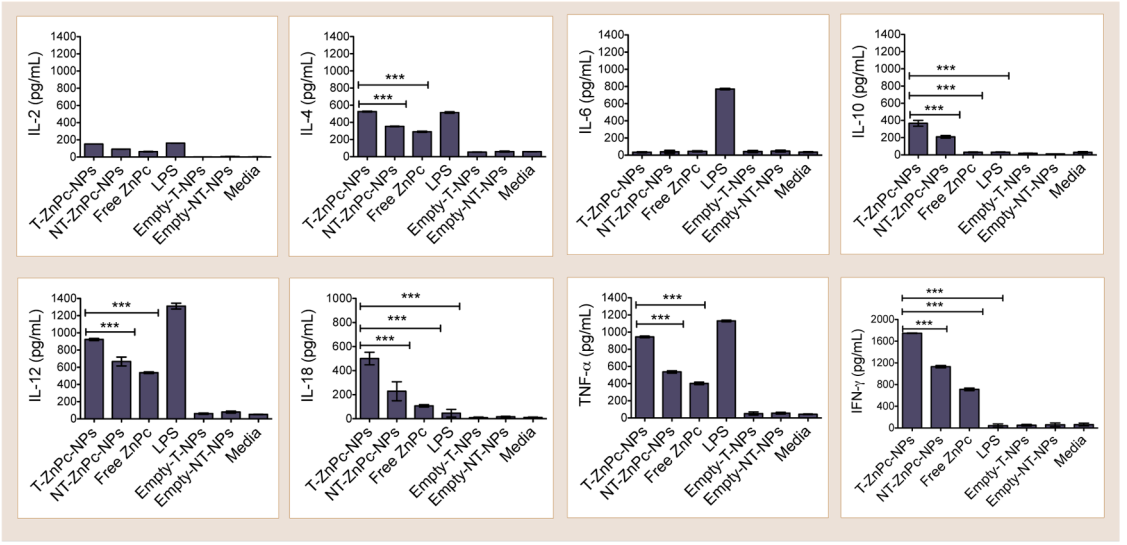

Figure 3. Cytokine production by BMDCs stimulated with cancer cell supernatants generated by treating MCF-7 cells with different constructs after PDT activation. Highly purified DCs were cultured at 0.5 × 10^6 cells/mL in the presence of a range of stimuli: MCF-7 cancer cells (0.5 × 10^6 cells/mL) treated with T-ZnPc-NP (20 nM with respect to ZnPc), NT-ZnPc-NP (20 nM with respect to ZnPc), ZnPc (20 nM), empty-T-NP (0.5 mg/mL with respect to polymer), empty-NT-NP (0.5 mg/mL with respect to polymer) for 4 h followed by photostimulation with 660 nm laser light for 1 min and further incubation in the dark for 12 h or stimulation with LPS (100 ng/mL). After 48 h, DC culture supernatants were harvested and assayed by ELISA. Data shown are based upon triplicate cultures of pooled cells sorted from three mice and are representative of four separate experiments. All data were expressed as mean ± SD (standard deviation). A one-way ANOVA with a *post hoc* Tukey test was used to identify significant differences among the groups with a p value < 0.001.

maturation, antigen presentation, and initiation of a robust adaptive immune response against cancer cells.

Mitochondria-Targeted-NP-Activated, Light-Stimulated Breast Cancer Antigens Drive *ex Vivo* IFN-γ Secretion from BMDCs. Several studies demonstrated activation of the host immune response by PDT following unknown mechanisms.[28] Secretion of IFN-γ by human T and NK cells in the adaptive immune responses against pathogens is well established,[29,30] but *ex vivo* generation of IFN-γ by DCs is still controversial.[31] We next assessed the activation of BMDCs by cancer cell antigens generated by treating MCF-7 cells with different constructs followed by light stimulation using an enzyme-linked immunosorbent assay (ELISA).[9] Treatment of MCF-7 cells with different constructs and light stimulation did not increase any cytokine levels (Figure S5). Cytokine production by monocytes or macrophages is not always reproducible. As a consequence of the purity of the isolated BMDC population, small numbers of NK or T cells contaminating macrophage cultures could mislead cytokine production. Therefore, we purified BMDCs isolated from C57BL/6 mice using an anti-CD11c microbead column (Figure S6). Control experiments by treating MCF-7 cells with different NPs followed by incubation of BMDCs with cancer cell supernatants in the dark did not show any induction of cytokine secretion (Figure S7). BMDCs activated with cancer cell supernatants from T-ZnPc-NP-treated and PDT-activated MCF-7 cells led to significant induction of pro-inflammatory cytokine secretion, which included IL-12, IL-18, and TNF-α as well as production of anti-inflammatory cytokines such as IL-4 and IL-10 (Figure 3) in a time-dependent manner (Figure S8) compared to BMDCs stimulated with supernatants of NT-ZnPc-NP or ZnPc-treated and light-activated cancer cells. Most importantly under these settings, BMDCs stimulated with cancer cell supernatants from T-ZnPc-NP-treated and light-activated MCF-7 cells produced IFN-γ to a greater extent than BMDCs treated with cancer cell supernatants generated with NT-ZnPc-NP or free ZnPC followed by PDT activation (Figure 3). BMDCs stimulated with supernatants from T-ZnPc-NP-treated PDT-activated cancer cells generated a marked IL-18 and IFN-γ response. In contrast addition of bacterial lipopolysaccharide (LPS) to BMDCs did not induce these two cytokines. Treatment of MCF-7 cells with T-LND-NPs, NT-LND-NPs, and free LND and stimulation of BMDCs with the LND-treated MCF-7 cancer cell supernatants did not show any immune-stimulatory cytokine production (Figure S9), further supporting that localization of mitochondria-acting PS using a NP system causes potent immune response; however similar strategies by directing mitochondria-acting chemotherapeutics such as LND using a delivery vehicle do not show any immune stimulation.[32,33] However, it should be noted that some chemotherapeutic agents act on the immune system to trigger a direct antitumor immune response.[34,35] Thus mitochondria-targeted PDT-generated supernatants provide a unique immune stimulation compared to chemotherapy. To investigate cancer cell specificity of IFN-γ production, we carried out experiments using cervical cancer HeLa cells (Figure S10). We observed that BMDCs stimulated with cell supernatants from HeLa cells

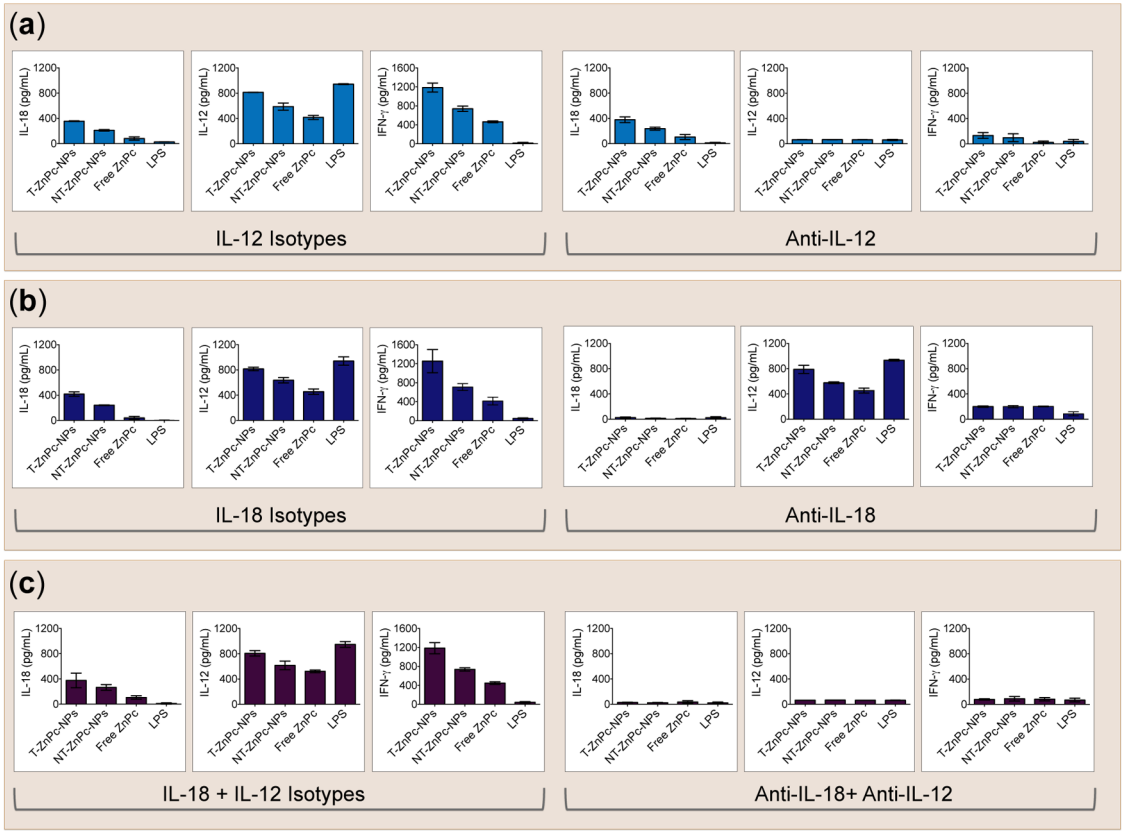

Figure 4. Combination of IL-12 and IL-18 is the source of IFN-γ. Purified BMDCs were treated with neutralizing antibodies against IL-12 and/or IL-18 cytokines, followed by incubation with different cancer cell supernatants or with LPS (100 ng/mL) for 48 h. MCF-7 cancer cells were incubated with T-ZnPc-NP (20 nM with respect to ZnPc), NT-ZnPc-NP (20 nM with respect to ZnPc), and ZnPc (20 nM) for 4 h followed by photostimulation with 660 nm laser light for 1 min and further incubation in the dark for 12 h. BMDCs were then harvested for ELISA.

treated with T-ZnPc-NPs, NT-ZnPc-NPs, and free ZnPc followed by PDT showed a very similar cytokine secretion prolife except for IL-18 and IFN-γ. This indicates that IFN-γ production by the activated BMDCs is dependent on the cancer cell type.

IL-12 and IL-18 Neutralization Abrogates T-ZnPc-NP-Treated and Light-Stimulated Cancer Cell Induced IFN-γ Production by BMDCs. A potential mechanism behind the remarkable immune response from the T-ZnPc-NP-treated MCF-7 vaccine lies in the ability of this tumor cell lysate to stimulate IFN-γ production from DCs by a unique combinatory secretion of IL-12 and IL-18. There are few reports demonstrating that a combination of IL-12 and IL-18 induces IFN-γ production in human DCs.[36,37] IL-12 secretion is a measure of functional DC maturation, and IL-18 is identified as an IFN-γ-inducing factor. The regulation of IL-18 secretion by the interaction of human DCs with T cells is known, but IL-18 secretion by mouse DCs is sparse.[38] Neutralization of either of IL-12 or IL-18 using neutralization antibodies completely eliminated the induction of IFN-γ secretion by the DCs activated with T-ZnPc-NP-treated and PDT-stimulated MCF-7 tumor cell supernatant compared to the BMDCs incubated with respective isotype controls (Figure 4). These data indicate that the IFN-γ secretion from DCs pulsed with T-ZnPc-NP-treated PDT-stimulated MCF-7 cancer cells was triggered by an autocrine effect of IL-12 and IL-18 (Figure 4). Our results showed that only conditioned media from breast cancer MCF-7 cells, and not cervical cancer HeLa cells, generated by treating with T-ZnPc-NPs upon photostimulation triggered the release of IL-18 and IFN-γ from BMDCs. Moreover, we found that IL-18 secretion varied strongly according to the use of the NP delivery vehicle, with mitochondria-targeted delivery yielding the highest IL-18 secretion, with reduced IL-18 secretion from NT-ZnPc-NPs or free ZnPc. These findings suggested that the extent that PDT-triggered secretion of IL-18 in DCs depends on the mechanism of apoptosis. Because the pattern of IL-18 secretion induced by the different NP-stimulated BMDCs resembled the pattern of IFN-γ from these BMDCs, we sought to identify the molecular mechanisms that might link IL-18 secretion, apoptosis, and IFN-γ production.

The secretion of IL-18 by DCs appeared to be a specific, caspase-1-mediated apoptosis effect, and a slow release of pro-IL-18 from the apoptotic cancer cells is required for DC activation to release IL-18.[39] This underlines the important role of caspase-1 in the activation of IL-18 and IFN-γ. Caspase-3 plays a central

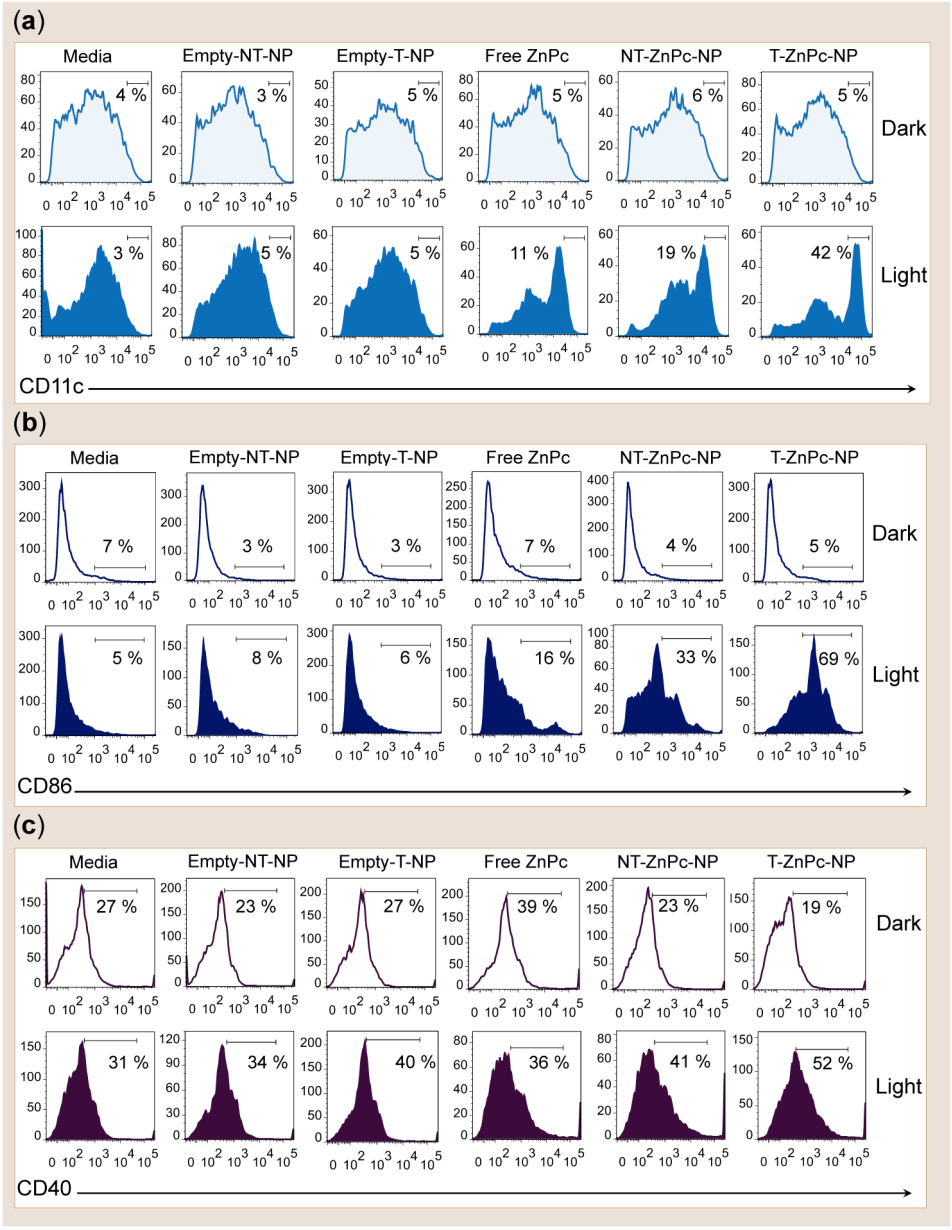

Figure 5. DC maturation assay. MCF-7 cell conditioned media treated with T-ZnPc-NPs followed by PDT stimulation induces expression of CD11c (a), CD86 (b), and CD40 (c) markers on DCs.

role in key apoptotic events. MCF-7 breast cancer cells lack caspase-3 protein,[40] yet they remain apoptosis responsive in our studies, suggesting an alternative mechanism. We believe that the mitochondria-targeted PDT in MCF-7 cells involved release of cytochrome *c*, a reduction in the $\Delta\psi_m$, and activation of different aspects of the caspase cascade,[41] and the possibility existed that caspase-1 might substitute for caspase-3. Thus, caspase-1 activation by the T-ZnPc-NPs upon light stimulation leads to the production of IL-18 from BMDCs, and subsequent activation by the unique combination of IL-12 and IL-18 might be responsible for the *ex vivo* induction of BMDCs to produce IFN-γ. This is further supported by the observation that HeLa cells with caspase-3 undergo a normal apoptotic pathway upon treatment with T-ZnPc-NPs and do not secrete IL-18 and IFN-γ (Figure S10). The precise mechanisms why T-ZnPc-NP-treated and PDT-stimulated breast cancer cells activate BMDCs to produce IFN-γ warrant further investigation.

Mitochondria-Targeted-NP-Treated, Light-Activated MCF-7 Cells Induce DC Maturation. Maturation and activation of DCs is a prerequisite for up-regulation of co-stimulatory molecules, enhancement of their APC function, and expression of chemokine receptors for migration to nodal T cell areas.[42] DCs undergo a number of phenotypical and functional changes, and DC-based therapy in humans demonstrated that DC maturation is a requirement for the induction of immunity.[43,44] In general, DC maturation involves a redistribution of major

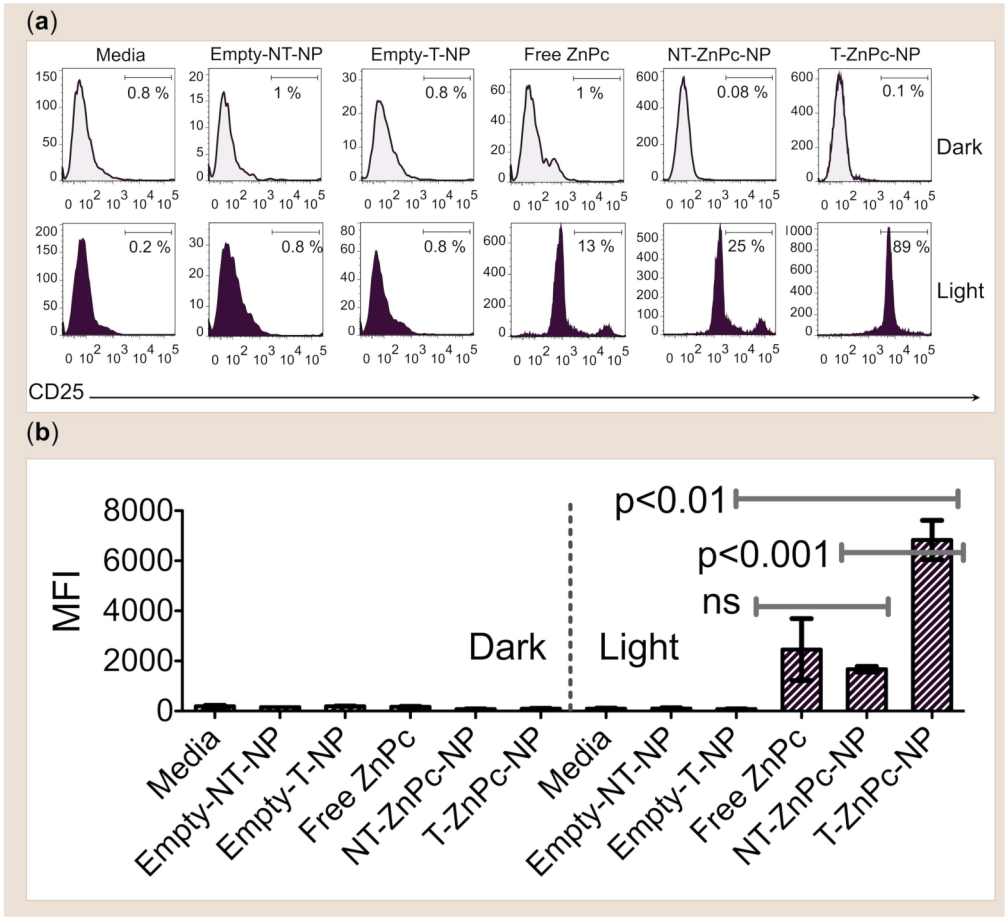

Figure 6. CD8 T cell activation assay. DCs exposed to supernatants of MCF-7 cells treated with different conjugates (20 nM with respect to ZnPc for T-ZnPc-NP, NT-ZnPc-NP, and free ZnPc; empty-NPs 0.5 mg/mL with respect to polymer) with or without light activate $CD8^+$ T cells. MCF-7 cells were incubated with the conjugates. Cancer cell supernatants were incubated with BMDCs. Activated BMDCs were incubated with $CD8^+$ T cells enriched from spleens of C57BL/6 mice. Cells were harvested to measure T cell activation by staining with antibodies against CD8 and CD25 (a), and median fluorescence intensities (MFIs) of CD25 were calculated using FlowJo software (b).

histocompatibility complex (MHC) from intracellular endocytic compartments to the DC surface, down-regulation of antigen internalization, an increase in the surface expression of co-stimulatory markers, secretion of chemokines, cytokines, and proteases, and surface expression of adhesion molecules and chemokine receptors.

Proper DC maturation by the PDT antigens is an integral part of PDT-based vaccine development. We studied the ability of the T-ZnPc-NP-treated PDT-stimulated MCF-7 cancer cell supernatant to induce maturation of BMDCs by performing phenotypic analysis using flow cytometry (Figure 5). BMDCs incubated with supernatant from T-ZnPc-NP-treated PDT-stimulated MCF-7 had a significant increase in the expression of CD11c compared with cells incubated with supernatant from PDT-stimulated MCF-7 cells treated with NT-ZnPc-NP or free ZnPc or DCs incubated with PDT-stimulated MCF-7 cells alone (Figure 5a). Expression of CD86 and CD40 surface markers on BMDCs was significantly increased when BMDCs were incubated with supernatants from MCF-7 cells treated with T-ZnPc-NPs then undergoing PDT stimulation compared to PDT-stimulated cell supernatants generated from NT-ZnPc-NPs (Figure 5b and c) or free ZnPc.

$CD8^+$ T Cell Activation. The inaugural step of T cell immunity involves interaction of naïve T cells with mature DCs.[45] iDCs are stimulators of T cells, and $CD8^+$ T cells play a crucial role in providing a full-strength adaptive immune response against cancer. Our observation that T-ZnPc-NP-treated, light-stimulated MCF-7 cell supernatant is efficient in driving DC maturation led us to hypothesize that BMDCs activated with this supernatant will show effective $CD8^+$ T cell activation. To probe this, $CD8^+$ T cells were incubated with BMDCs pre-exposed to the cancer cell supernatants treated with NPs and pulsed with laser. CD25 was significantly up-regulated on the $CD8^+$ T cells that were cocultured with the BMDCs stimulated with T-ZnPc-NP-treated, light-activated cancer cell media. In comparison, $CD8^+$ T cells incubated with BMDCs exposed to MCF-7 cancer cell supernatants that received NT-ZnPc-NP or free ZnPc showed significantly reduced T cell activation (Figure 6). This remarkable ability of

BMDCs stimulated with T-ZnPc-NP-treated, light-activated tumor cell supernatant to induce high surface expression of CD25 on $CD8^+$ T cells indicated that this mitochondria-targeted, PS-containing NP has the opportunity to be explored further for possible vaccine applications.

CONCLUSIONS

In conclusion, we demonstrate an exceptional potency of mitochondria-targeted-NP-based, light-activated breast cancer cell antigens to uniquely stimulate DCs for cancer immunotherapy. A major advantage of activating DCs *ex vivo* to produce IFN-γ is that these activated DCs can be produced in bulk quantities, *ex vivo* culture conditions can be carefully controlled, and DC quality can be checked before the cells are administered to the patient. Our findings encourage the use of mitochondria-targeted-NP delivery systems to deliver mitochondria-acting PS for generation of tumor cell antigens to activate DCs *ex vivo* for potential interactive innate/acquired immune response with relevance to and impact on health and disease.

EXPERIMENTAL SECTION

Materials and Instrumentations. Details of the materials and instruments used can be found in the Supporting Information.

Cell Line and Cell Culture. Human cervical cancer HeLa, human breast adenocarcinoma MCF-7, and primary hMSC cells were procured from the American Type Culture Collection (ATCC). HeLa and MCF-7 cells were grown at 37 °C in 5% CO_2 in Dulbecco's modified Eagle medium (DMEM) medium supplemented with 10% fetal bovine serum (FBS) and 1% penicillin/streptomycin. MSC cells were grown in MSC basal medium supplemented with MSC growth kit low-serum components and 2% FBS. Cells were passed every 3 to 4 days and restarted from frozen stocks upon reaching pass number 20 for MCF-7 and HeLa and 3 for MSC.

Animals. Animals were obtained from Jackson Laboratory and handled in accordance with "The Guide for the Care and Use of Laboratory Animals" of the Association for Accreditation of Laboratory Animal Care (AAALAC), Animal Welfare Act (AWA), and other applicable federal and state guidelines. All animal work presented here was approved by the Institutional Animal Care and Use Committee (IACUC) of the University of Georgia (UGA).

Generation of Immature BMDCs. BMDCs were isolated from 6- to 8-week-old C57BL/6 mice. Mice were euthanized, and bone marrows were isolated by flushing mouse femurs in Roswell Park Memorial Institute (RPMI) 1640 medium. The harvested cells were centrifuged at 1250 rpm for 10 min, and the resulting pellet was resuspended in 2 mL of ice-cold buffer to lyse erythrocytes. The cells were counted, resuspended, and transferred to Petri dishes at a final concentration of 1.5×10^6 cells/mL. To this culture was added granulocyte-macrophage colony-stimulating factor (20 ng/mL) to generate BMDCs. Media was changed on days 2 and 4. On day 6 cells were processed further to obtain pure DC population by subjecting cells to MACS bead purification using anti-CD11c antibody as per the manufacturer's instructions. DC purity was tested by incubating BMDCs with LPS (100 ng/mL), and the surface expression of CD11c was measured. DCs were found to be >90% pure.

Synthesis of Empty Targeted and Nontargeted NPs. Empty NPs were synthesized by the nanoprecipitation method, the details of which can be found in the Supporting Information. DLS measurements were carried out to determine size, polydispersity index (PDI), and zeta potential of the NPs. The morphology of the NPs was characterized using TEM.

Synthesis of ZnPc or LND-Encapsulated NPs. NPs were synthesized by the nanoprecipitation method. Briefly, PLGA-*b*-PEG-OH or PLGA-*b*-PEG-TPP (50 mg/mL) in dimethylformamide (DMF) was mixed with a predefined amount of ZnPc (10 mg/mL in DMF) and diluted with DMF to a final polymer concentration of 5 mg/mL. This mixture was added dropwise to nanopure water with constant stirring. The NPs were stirred for 2 h at room temperature. Organic solvent was removed by washing three times using a 100 kDa cutoff Amicon filtration membrane. The NPs were resuspended in nanopure water and stored at 4 °C until further use. DLS measurements were carried out to determine size, PDI, and zeta potential. NPs were characterized using TEM at an acceleration voltage of 200 kV. The TEM samples were prepared by depositing 8 μL of the NPs (5 mg/mL) onto a 200-mesh carbon-coated copper grid. Samples were blotted away after 15 min, and grids were negatively stained with sterile 2% (w/v) uranyl acetate aqueous solution for 15 min. ZnPc loading and EE were determined by dissolving the polymeric core and quantifying the amount of ZnPc in the NPs using high-performance liquid chromatography (HPLC) (wavelength used: 670 nm).

For LND-encapsulated NPs, PLGA-*b*-PEG-OH or PLGA-*b*-PEG-TPP (50 mg/mL in DMF) was mixed with a predefined amount of LND (10 mg/mL in DMSO) and diluted with DMF to a final polymer concentration of 5 mg/mL. This mixture was added dropwise to nanopure water with constant stirring. The NPs were stirred for 2 h at room temperature. Organic solvent was removed by washing three times using a 100 kDa cutoff Amicon filtration membrane. The NPs were resuspended in nanopure water and stored at 4 °C until further use. DLS measurements were carried out to determine size, PDI, and zeta potential. LND loading and EE were determined by dissolving the polymeric core and quantifying the amount of LND in the NPs using HPLC (wavelength used: 297 nm).

Determination of ZnPc and LND Loading and Encapsulation Efficiency. Loading and EE of ZnPc and LND in NPs were calculated by dissolving the polymeric core by mixing equal portions of the NP solution and 0.1 M NaOH, followed by dilution with a 50:50 water/acetonitrile mixture and subsequent HPLC analysis. Drug loading is defined as the mass fraction of drug in the NPs, whereas EE is the fraction of initial drug that is encapsulated in the NPs.

Cytotoxicity Assay. The cytotoxic behavior of all the NPs was evaluated using the MTT assay against MCF-7, HeLa, and MSC cells. Cells (2000 cells/well) were seeded on a 96-well plate in 100 μL of DMEM medium and incubated for 24 h. The cells were treated with NPs at varying concentrations (with respect to ZnPc) and incubated for 4 h at 37 °C. The cells were then irradiated with 660 nm laser (power 20.0 mV) light with fiber optics for 1 min per well. Irradiated cells were incubated for 12 h at 37 °C, followed by a media change for all cells, and the cells were incubated for an additional 60 h. The cells were then treated with 20 μL of MTT (5 mg/mL in PBS) for 5 h. The medium was removed, the cells were lysed with 100 μL of DMSO, and the absorbance of the purple formazan was recorded at 550 nm using a Bio-Tek Synergy HT microplate reader. Each well was performed in triplicate. All experiments were repeated three times. Cytotoxicity was expressed as mean percentage increase relative to the unexposed control $\pm$ SD. Control values were set at 0% cytotoxicity or 100% cell viability. Cytotoxicity data (where appropriate) were fitted to a sigmoidal curve, and a three-parameter logistic model was used to calculate the IC_{50}, which is the concentration of agent causing 50% inhibition in comparison to untreated controls. The mean IC_{50} is the concentration of agent that reduces cell growth by 50% under the experimental conditions and is the average from at least three independent measurements that were reproducible and statistically significant. The IC_{50} values were reported at $\pm$95% confidence intervals. This analysis was performed with GraphPad Prism (San Diego, CA, USA).

Apoptosis Detection. MCF-7 cells were seeded at a density of 1×10^6 on each well of a six-well plate and allowed to grow overnight. Cells were treated with 1 μM ZnPc, 0.5 mg/mL empty NPs, or 1 μM targeted and nontargeted ZnPc encapsulated NPs, incubated for 4 h, and then irradiated with a 660 nm laser (1 min/well). As a control, the same formulations were added without light irradiation. The cells were further incubated at 37 °C overnight followed by trypsinization. The cells were repeatedly washed and centrifuged at 1800 rpm for 3 min, and the supernatants were discarded. Cell density was determined, and cells were resuspended in annexin-binding buffer to $\sim 1 \times 10^6$ cells/mL, preparing a sufficient volume to have 100 μL per assay. To 100 μL of cell suspension were added 5 μL of Alexa Fluor 488 annexin V and 1 μL of 100 μg/mL PI working solution, and the solution was incubated for 15 min at room temperature. After the incubation period, 400 μL of annexin-binding buffer was added to each sample, samples were gently mixed keeping the samples on ice, and the samples were analyzed on the flow cytometer immediately.

Antitumor Immunity Study. MCF-7 or HeLa cells were plated at a concentration of 0.5×10^6 cells/mL in six-well plates and allowed to grow for 12 h. On the next day, the cells were incubated with 20 nM ZnPc, 0.5 mg/mL empty NPs, or 20 nM targeted and nontargeted ZnPc encapsulated NPs for 4 h and irradiated with 660 nm light for 1 min per well. As a control, the same doses were incubated without light irradiation. Cells were left in the culture overnight at 37 °C, and PDT supernatants were added to freshly prepared BMDCs (0.5×10^6 cells/mL). DCs were incubated with supernatants at 37 °C in a time-dependent manner (12, 24, and 48 h) for MCF-7 cells and 48 h for HeLa cells. Additionally LPS alone (100 ng/mL) was added to the DC cultures. The DCs were centrifuged at 1800 rpm for 3 min, and ELISA assays were performed on the supernatants against the cytokines IL-2, IL-4, IL-6, IL-10, IL-12, IL-18, TNF-α, and IFN-γ according to the manufacturer's protocol. Briefly, antibody-coated plates were blocked with 10% FBS in PBS for 1 h at room temperature followed by washings. Afterward, DC supernatants were incubated on the plates for 1 h at room temperature. This was immediately followed by washings and sequential incubations with the cytokine−biotin conjugate and streptavidin working solution. Finally, the substrate reagent containing 3,3′,5,5′-tetramethylbenzidine (100 μL) was added to each well, the plates were incubated for 30 min, and the reaction was stopped by adding 50 μL of stop solution containing 0.1 M H_2SO_4. The absorbance was recorded at 450 nm using a BioTek Synergy HT well plate reader.

Neutralization of IL-12 and IL-18. Purified BMDCs were treated with neutralizing antibodies against IL-12 (5 μg/mL) and/or IL-18 (1 μg/mL) cytokines for 18 h, followed by incubation with different NP-treated and PDT-activated MCF-7 cancer cell supernatants for 48 h. MCF-7 cells (0.5×10^6 cells/mL) were incubated with T-ZnPc-NP (20 nM), NT-ZnPc-NP (20 nM), or free ZnPc (20 nM) for 4 h, activated by PDT for 1 min as described before. Supernatants from the BMDCs were analyzed by ELISA to evaluate the levels of IL-12, IL-18, and IFN-γ. BMDCs were also harvested to stain for surface marker CD11c followed by intracellular staining of IFN-γ. Cells were acquired on a flow cytometer, and data were analyzed on FlowJo software. Production of IFN-γ was analyzed in $CD11c^+$ gated population.

DC Maturation and T Cell Activation Assays. For the DC maturation assay, cancer cell supernatants obtained after treatment of MCF-7 cells with different conjugates followed by PDT were incubated with BMDCs for 24 h at 37 °C. Cells were harvested and stained with antibodies against surface markers CD11c, CD86, and MHCII for 1 h on ice. Cells were washed in stain buffer and acquired on a BD LSRII flow cytometer. Data obtained were analyzed using FlowJo software. To study $CD8^+$ T cell activation, BMDCs, incubated with cancer cell supernatants, were treated with different conjugates followed by PDT as described above and were further incubated with $CD8^+$ T cells purified from splenocytes of naïve C57BL/6 mice using the MACS bead negative selection method for 72 h. Cells were harvested, and $CD8^+$ T cell activation was studied by staining the cells with antibodies against CD8 and CD25 surface markers. Cells were then acquired on a flow cytometer.

Conflict of Interest: The authors declare no competing financial interest.

Supporting Information Available: Additional methods, figures, and tables. This material is available free of charge *via* the Internet at http://pubs.acs.org.

Acknowledgment. This work was supported by a start-up grant from the National Institutes of Health (P30 GM 092378) to UGA, by the Office of the Vice President for Research, UGA, to S.D., and by a grant from the National Institutes of Health (NIH AI056484) to D.H. We thank Dr. Nagesh Kolishetti for helpful discussions and critical reading of the manuscript.

REFERENCES AND NOTES

1. Swann, J. B.; Smyth, M. J. Immune Surveillance of Tumors. *J. Clin. Invest.* **2007**, *117*, 1137–1146.
2. Mellman, I.; Coukos, G.; Dranoff, G. Cancer Immunotherapy Comes of Age. *Nature* **2011**, *480*, 480–489.
3. Tacken, P. J.; de Vries, I. J. M.; Torensma, R.; Figdor, C. G. Dendritic-Cell Immunotherapy: From *ex Vivo* Loading to *in Vivo* Targeting. *Nat. Rev. Immunol.* **2007**, *7*, 790–802.
4. Timmerman, J. M.; Levy, R. Dendritic Cell Vaccines for Cancer Immunotherapy. *Annu. Rev. Med.* **1999**, *50*, 507–529.
5. Chang, D. H.; Dhodapkar, M. V. Dendritic Cells and Immunotherapy for Cancer. *Int. J. Hematol.* **2003**, *77*, 439–443.
6. Nestle, F. O.; Farkas, A.; Conrad, C. Dendritic-Cell-Based Therapeutic Vaccination against Cancer. *Curr. Opin. Immunol.* **2005**, *17*, 163–169.
7. Garg, A. D.; Nowis, D.; Golab, J.; Agostinis, P. Photodynamic Therapy: Illuminating the Road from Cell Death towards Anti-Tumour Immunity. *Apoptosis* **2010**, *15*, 1050–1071.
8. Castano, A. P.; Mroz, P.; Hamblin, M. R. Photodynamic Therapy and Anti-Tumour Immunity. *Nat. Rev. Cancer* **2006**, *6*, 535–545.
9. Marrache, S.; Choi, J. H.; Tundup, S.; Zaver, D.; Harn, D. A.; Dhar, S. Immune Stimulating Photoactive Hybrid Nanoparticles for Metastatic Breast Cancer. *Integr. Biol.* **2013**, *5*, 215–223.
10. Farokhzad, O. C.; Jon, S. Y.; Khademhosseini, A.; Tran, T. N. T.; LaVan, D. A.; Langer, R. Nanoparticle-Aptamer Bioconjugates: A New Approach for Targeting Prostate Cancer Cells. *Cancer Res.* **2004**, *64*, 7668–7672.
11. Farokhzad, O. C.; Cheng, J.; Teply, B. A.; Sherifi, I.; Jon, S.; Kantoff, P. W.; Richie, J. P.; Langer, R. Targeted Nanoparticle-Aptamer Bioconjugates for Cancer Chemotherapy *in Vivo*. *Proc. Natl. Acad. Sci. U.S.A.* **2006**, *103*, 6315–6320.
12. Soppimath, K. S.; Aminabhavi, T. M.; Kulkarni, A. R.; Rudzinski, W. E. Biodegradable Polymeric Nanoparticles as Drug Delivery Devices. *J. Controlled Release* **2001**, *70*, 1–20.
13. Gu, F.; Zhang, L.; Teply, B. A.; Mann, N.; Wang, A.; Radovic-Moreno, A. F.; Langer, R.; Farokhzad, O. C. Precise Engineering of Targeted Nanoparticles by Using Self-Assembled Biointegrated Block Copolymers. *Proc. Natl. Acad. Sci. U.S.A.* **2008**, *105*, 2586–2591.
14. Dhar, S.; Kolishetti, N.; Lippard, S. J.; Farokhzad, O. C. Targeted Delivery of a Cisplatin Prodrug for Safer and More Effective Prostate Cancer Therapy *in Vivo*. *Proc. Natl. Acad. Sci. U.S.A.* **2011**, *108*, 1850–1855.
15. Marrache, S.; Dhar, S. Biodegradable Synthetic High-Density Lipoprotein Nanoparticles for Atherosclerosis. *Proc. Natl. Acad. Sci. U.S.A.* **2013**, *110*, 9445–9450.
16. Marrache, S.; Pathak, R. K.; Darley, K. L.; Choi, J. H.; Zaver, D.; Kolishetti, N.; Dhar, S. Nanocarriers for Tracking and Treating Diseases. *Curr. Med. Chem.* **2013**, *20*, 3500–3514.
17. Smith, R. A. J.; Porteous, C. M.; Gane, A. M.; Murphy, M. P. Delivery of Bioactive Molecules to Mitochondria *in Vivo*. *Proc. Natl. Acad. Sci. U.S.A.* **2003**, *100*, 5407–5412.
18. Marrache, S.; Dhar, S. Engineering of Blended Nanoparticle Platform for Delivery of Mitochondria-Acting Therapeutics. *Proc. Natl. Acad. Sci. U.S.A.* **2012**, *109*, 16288–16293.
19. Redmond, R. W.; Kochevar, I. E. Spatially Resolved Cellular Responses to Singlet Oxygen. *Photochem. Photobiol.* **2006**, *82*, 1178–1186.

20. Skovsen, E.; Snyder, J. W.; Lambert, J. D.; Ogilby, P. R. Lifetime and Diffusion of Singlet Oxygen in a Cell. *J. Phys. Chem. B* **2005**, *109*, 8570–8573.
21. Dhar, S.; Gu, F. X.; Langer, R.; Farokhzad, O. C.; Lippard, S. J. Targeted Delivery of Cisplatin to Prostate Cancer Cells by Aptamer Functionalized Pt(IV) Prodrug-PLGA-PEG Nanoparticles. *Proc. Natl. Acad. Sci. U.S.A.* **2008**, *105*, 17356–17361.
22. Kolishetti, N.; Dhar, S.; Valencia, P. M.; Lin, L. Q.; Karnik, R.; Lippard, S. J.; Langer, R.; Farokhzad, O. C. Engineering of Self-Assembled Nanoparticle Platform for Precisely Controlled Combination Drug Therapy. *Proc. Natl. Acad. Sci. U.S.A.* **2010**, *107*, 17939–17944.
23. Floridi, A.; Paggi, M. G.; Marcante, M. L.; Silvestrini, B.; Caputo, A.; Demartino, C. Lonidamine, a Selective Inhibitor of Aerobic Glycolysis of Murine Tumor Cells. *J. Natl. Cancer I* **1981**, *66*, 497–499.
24. Davis, S.; Weiss, M. J.; Wong, J. R.; Lampidis, T. J.; Chen, L. B. Mitochondrial and Plasma Membrane Potentials Cause Unusual Accumulation and Retention of Rhodamine 123 by Human Breast Adenocarcinoma-Derived MCF-7 Cells. *J. Biol. Chem.* **1985**, *260*, 13844–13850.
25. Chen, L. B. Mitochondrial Membrane Potential in Living Cells. *Annu. Rev. Cell. Biol.* **1988**, *4*, 155–181.
26. Steinman, R. M.; Inaba, K.; Turley, S.; Pierre, P.; Mellman, I. Antigen Capture, Processing, and Presentation by Dendritic Cells: Recent Cell Biological Studies. *Hum. Immunol.* **1999**, *60*, 562–567.
27. Buytaert, E.; Dewaele, M.; Agostinis, P. Molecular Effectors of Multiple Cell Death Pathways Initiated by Photodynamic Therapy. *BBA-Rev. Cancer* **2007**, *1776*, 86–107.
28. Mroz, P.; Hashmi, J. T.; Huang, Y. Y.; Lange, N.; Hamblin, M. R. Stimulation of Anti-tumor Immunity by Photodynamic Therapy. *Expert Rev. Clin. Immunol.* **2011**, *7*, 75–91.
29. Papadakis, K. A.; Prehn, J. L.; Landers, C.; Han, Q. W.; Luo, X.; Cha, S. C.; Wei, P.; Targan, S. R. TL1A Synergizes with IL-12 and IL-18 to Enhance IFN-Gamma Production in Human T Cells and NK Cells. *J. Immunol.* **2004**, *172*, 7002–7007.
30. Tominaga, K.; Yoshimoto, T.; Torigoe, K.; Kurimoto, M.; Matsui, K.; Hada, T.; Okamura, H.; Nakanishi, K. IL-12 Synergizes with IL-18 or IL-1 beta for IFN-Gamma Production from Human T Cells. *Int. Immunol.* **2000**, *12*, 151–160.
31. Fricke, I.; Mitchell, D.; Mittelstadt, J.; Lehan, N.; Heine, H.; Goldmann, T.; Bohle, A.; Brandau, S. Mycobacteria Induce IFN-Gamma Production in Human Dendritic Cells *via* Triggering of TLR2. *J. Immunol.* **2006**, *176*, 5173–5182.
32. Oliver, R. T. D.; Nouri, A. M. E. T Cell Immune Response to Cancer in Humans and Its Relevance for Immunodiagnosis and Therapy. *Cancer Surv.* **1992**, *13*, 173–204.
33. Mokyr, M. B.; Dray, S. Interplay between the Toxic Effects of Anticancer Drugs and Host Antitumor Immunity in Cancer Therapy. *Cancer Invest.* **1987**, *5*, 31–38.
34. Menard, C.; Martin, F.; Apetoh, L.; Bouyer, F.; Ghiringhelli, F. Cancer Chemotherapy: Not Only a Direct Cytotoxic Effect, but Also an Adjuvant for Antitumor Immunity. *Cancer Immunol. Immunother.* **2008**, *57*, 1579–1587.
35. Mattarollo, S. R.; Loi, S.; Duret, H.; Ma, Y.; Zitvogel, L.; Smyth, M. J. Pivotal Role of Innate and Adaptive Immunity in Anthracycline Chemotherapy of Established Tumors. *Cancer Res.* **2011**, *71*, 4809–4820.
36. Robinson, C. M.; O'Dee, D.; Hamilton, T.; Nau, G. J. Cytokines Involved in Interferon-Gamma Production by Human Macrophages. *J. Innate Immun.* **2010**, *2*, 56–65.
37. Darwich, L.; Coma, G.; Pena, R.; Bellido, R.; Blanco, E. J.; Este, J. A.; Borras, F. E.; Clotet, B.; Ruiz, L.; Rosell, A.; *et al*. Secretion of Interferon-Gamma by Human Macrophages Demonstrated at the Single-Cell Level after Costimulation with Interleukin (IL)-12 Plus IL-18. *Immunology* **2009**, *126*, 386–393.
38. Gardella, S.; Andrei, C.; Costigliolo, S.; Poggi, A.; Zocchi, M. R.; Rubartelli, A. Interleukin-18 Synthesis and Secretion by Dendritic Cells Are Modulated by Interaction with Antigen-Specific T Cells. *J. Leukocyte Biol.* **1999**, *66*, 237–241.
39. Dreher, D.; Kok, M.; Obregon, C.; Kiama, S. G.; Gehr, P.; Nicod, L. P. Salmonella Virulence Factor SipB Induces Activation and Release of IL-18 in Human Dendritic Cells. *J. Leukocyte Biol.* **2002**, *72*, 743–751.
40. Mooney, L. M.; Al-Sakkaf, K. A.; Brown, B. L.; Dobson, P. R. Apoptotic Mechanisms in T47D and MCF-7 Human Breast Cancer Cells. *Br. J. Cancer* **2002**, *87*, 909–917.
41. Benjamin, C. W.; Hiebsch, R. R.; Jones, D. A. Caspase Activation in MCF7 Cells Responding to Etoposide Treatment. *Mol. Pharmacol.* **1998**, *53*, 446–50.
42. Banchereau, J.; Briere, F.; Caux, C.; Davoust, J.; Lebecque, S.; Liu, Y. T.; Pulendran, B.; Palucka, K. Immunobiology of Dendritic Cells. *Annu. Rev. Immunol.* **2000**, *18*, 767–811.
43. de Vries, I. J. M.; Lesterhuis, W. J.; Scharenborg, N. M.; Engelen, L. P. H.; Ruiter, D. J.; Gerritsen, M. J. P.; Croockewit, S.; Britten, C. M.; Torensma, R.; Adema, G. J.; *et al*. Maturation of Dendritic Cells Is a Prerequisite for Inducing Immune Responses in Advanced Melanoma Patients. *Clin. Cancer Res.* **2003**, *9*, 5091–5100.
44. Dhodapkar, M. V.; Steinman, R. M.; Krasovsky, J.; Munz, C.; Bhardwaj, N. Antigen-Specific Inhibition of Effector T Cell Function in Humans after Injection of Immature Dendritic Cells. *J. Exp. Med.* **2001**, *193*, 233–238.
45. Lanzavecchia, A.; Sallusto, F. Regulation of T Cell Immunity by Dendritic Cells. *Cell* **2001**, *106*, 263–266.